Image Quality and Dose Comparison of 3 Mobile Intraoperative Three-Dimensional Imaging Systems in Spine Surgery

Norah Foster[1,6], Christopher Shaffrey[1], Avery Buchholz[2], Raymond Turner[4], Lexie Zidanyue Yang[5], Donna Niedzwiecki[5], Allen Goode[3]

■ OBJECTIVE: **To evaluate radiation exposure and image quality (IQ) for 3 intraoperative imaging systems (Airo TruCT, Cios Spin, O-arm) using varying radiation dose settings in a single cadaveric model.**

■ METHODS: **Axial images of L4-5 instrumentation were obtained using 3 manufacturer dose protocols for each system. Measurements included scattered radiation dose, subjective and objective IQ, and estimates of patient effective dose (ED). Four images per system were selected at each dose level. Using the Likert scale (1 = best, 5 = worst), 9 reviewers rated the same 36 images. Objective IQ measures included the degree of streak artifacts (lines with incorrect data from metal objects) in each image. A composite figure of merit was derived based on ED and subjective and objective scores.**

■ RESULTS: **The best subjective IQ scores were 1.44 (Cios Spin medium dose), 1.78 (Cios Spin high dose) and 2.22 (Airo TruCT low dose). The best objective IQ scores were 87.3 (Airo TruCT) and 89.1 (Cios Spin). ED low-dose results in mSv included 1.6 (Airo TruCT), 1.9 (Cios Spin), and 3.3 (O-arm). ED high-dose results in mSv included 4.6 (Cios Spin), 9.7 (Airo TruCT), and 9.9 (O-arm). Scatter radiation measurements for low dose in μGy included 21.9 (Cios Spin), 31.8 (Airo TruCT), and 33.9 (O-arm). Scatter radiation for high dose in μGy included 55.9 (Cios Spin), 104.5 (O-arm), and 200 (Airo TruCT). The best figure of merit score was for the Airo TruCT low dose, followed by Cios Spin medium dose and high dose.**

■ CONCLUSIONS: **Selection of intraoperative imaging systems requires a greater understanding of the risks and benefits of radiation exposure and IQ.**

INTRODUCTION

Advancements in spine surgery imaging capabilities have progressed from serial radiography and C-arm fluoroscopy to two- and three-dimensional imaging, with the additional capability of navigation enabling real-time feedback. Imaging permits the localization of levels, assessment of alignment or reduction, and confirmation of proper implant placement and decompression. Although surgeons have a multitude of intraoperative imaging modalities from which to choose, each has advantages and disadvantages.

Patient and provider safety mandates consideration of radiation exposure in diagnostic and therapeutic procedures. Current

Key words
- 3D imaging
- Effective dose
- Image quality
- Intraoperative imaging
- Radiation dose
- Scatter dose

Abbreviations and Acronyms
ALARA: As low as reasonably achievable
CBCT: Cone-beam computed tomography
CI: Confidence interval
CT: Computed tomography
CTDI: Computed tomography dose index
ED: Effective dose
FOM: Figure of merit
IQ: Image quality
Ka,r: Reference point air kerma
SD: Standard deviation

From the [1]Department of Neurosurgery and Orthopaedic Surgery, Duke University School of Medicine, Durham, North Carolina; Departments of [2]Neurosciences Surgery and [3]Radiology and Medical Imaging, University of Virginia, Charlottesville, Virginia; [4]Department of Neurosurgery, Prisma Health, Greenville, South Carolina; and [5]Department of Biostatistics and Bioinformatics, Duke University, Durham, North Carolina, USA

[6]Present address: Department of Orthopaedic Surgery, Premier Orthopaedics, 2400 Miami Valley Dr, Suite 160, Centerville, OH 45459, USA.

*To whom correspondence should be addressed: Norah Foster, M.D.
[E-mail: snorahppp@gmail.com]*

*Citation: World Neurosurg. (2022) 160:e142-e151.
https://doi.org/10.1016/j.wneu.2021.12.103*

*Journal homepage: **www.journals.elsevier.com/world-neurosurgery***

*Available online: **www.sciencedirect.com***

guidelines set out by the National Council on Radiation Protection and Measurement limit the maximum annual radiation cumulative whole-body dose to 50 mSv for occupational workers.[1,2] For context, a chest x-ray is a 0.1-mSv exposure.[3] However, no radiation exposure limit exists for patients.

The fundamental principle for radiation protection is ALARA (as low as reasonably achievable). Studies show that surgeon radiation exposure is 12 times greater in spine surgery than in other orthopedic specialties[4] owing to patient torso thickness and the proximity of the surgeon to the radiation source.[5] Recommended dose limits are in place by regulatory agencies to prevent acute and cumulative (deterministic) effects and to reduce the probability of stochastic effects in medical professionals and patients.

MATERIALS AND METHODS

Three commercially available mobile imaging devices approved by the Food and Drug Administration were compared: O-arm (Medtronic, Minneapolis, Minneapolis, USA), Cios Spin (Siemens Medical Solutions, Malvern, Pennsylvania, USA), and Airo TruCT (Stryker, Kalamazoo, Michigan, USA). The O-arm provides intraoperative two-dimensional fluoroscopic and three-dimensional cone-beam computed tomography (CBCT) image guidance for orthopedic and neurosurgical procedures. The Cios Spin is a mobile C-arm that provides two-dimensional fluoroscopic and cine imaging and three-dimensional CBCT. The Airo TruCT is a mobile intraoperative 32- slice computed tomography (CT) scanner with an integrated table holder whose gantry pans along the patient independently of the patient and operating room table. System specifications are detailed in Table 1.

Surgical screw placement was performed at Duke University Hospital (Durham, North Carolina, USA). A fresh torso cadaver (female, age 59, body mass index 27.54) was placed prone on an Airo Trumpf operating room table (Hill-Rom, Chicago, Illinois, USA). An open midline incision was made over the lumbar spine. All soft tissue and paraspinal musculature were dissected laterally to the transverse processes to mimic the typical surgical exposure. Using anatomic landmarks and standard surgical techniques, the junction of the lateral border of the facet and midpoint of the transverse process were chosen as the starting points for pedicle instrumentation. The entry point was decorticated with a rongeur. The pedicle was cannulated with a curved pedicle probe. A ball-tipped probe was used to palpate the screw trajectory and provide tactile feedback of any pedicle wall breaches. Each hole was tapped before screw insertion and subsequently reevaluated for breach with the ball-tipped probe. Titanium pedicle screws (5.5 mm × 40 mm) (Reline System; NuVasive, San Diego, California, USA) were subsequently placed at L4 and L5 bilaterally. Implant placement was confirmed using standard fluoroscopy (OEC 9800; GE Healthcare, Chicago, Illinois, USA).

Table 1. System Specifications for Each System Tested

	Airo TruCT	Cios Spin	O-Arm
Size C-arm, L × W × H, cm	196 × 38 × 197	220 × 84 × 181	281 × 8 × 302
Footprint, m^2	1.5 (transport mode)	1.4	1.7
Free space/bore, cm	107 bore	93.6 free space	96.5 bore
3D volume, cm^3	50 × 100	16 × 16 × 16	20 × 15
C-arm weight, kg	1068	399	925.8
Detector	32 slice × 2.0 mm	30 cm × 30 cm	30 cm × 40 cm
Generator power, kW	30	25	32
OR table	Integrated Trumpf table	Radiolucent table	Radiolucent table

L, length; W, width; H, height; 3D, three-dimensional; OR, operating room.

Following surgical screw placement, 3 CT scans were performed using Airo TruCT per the parameters in Table 2. The manufacturer's maximum dose spine/lumbar program served as an indicator of the best image quality (IQ) condition, followed by the medium- and lower-dose protocols used at Duke University Health System. The cadaver was transported to UVA Health (Charlottesville, Virginia, USA) and imaged the next day on a radiolucent operating room table using the O-arm and Cios Spin. Alignment scans were acquired, followed by 3 cone-beam acquisitions on the Cio Spin and O-arm with each system, using the parameters in Table 2. Scan parameters for the 3 units were chosen from highest available, a medium level, and a lower level of those clinically used, referred to as high, medium, and low in this study. Reconstructed two-dimensional axial images were obtained for all 3 dose protocols on all units. No artifact reduction algorithms were used on any device.

Objective IQ

Metallic screws introduce streak artifacts in CT and CBCT that extend beyond the screw. The artifact is due to the metal screws attenuating radiation, introducing streaks during image reconstruction. Slices with more artifacts should have greater standard deviations (SDs) owing to the abrupt soft tissue/streak changes in the pixel data, resulting in inferior IQ. To quantify the artifact, a custom software program was written in IDL (Harris Geospatial Solutions, Broomfield, Colorado, USA). For each device, a central point ventral to the spine was selected on axial slices containing both screws. A semicircle was placed at a 50-mm radius around the screw. This radius was chosen to avoid the air interface introduced by the surgery. The IDL program recorded individual pixel values along the semicircle and placed them in an array for each axial slice, 2.5 cm above and below each screw, at each level. Using the method described by Komlosi et al.,[6,7] SDs were determined for the pixel array for each axial slice, yielding an SD for each slice.

Scatter Dose Measurement

Because each device differs in classification (CBCT vs. CT) and reports dose differently, scatter dose was used as a unifying measurement for operator dose. A 60-cm^3 volume ion chamber (10 x 60; RadCal, Monrovia, California, USA) was mounted at the central height of the cadaver placed at 1 m from each system isocenter at 45° from the centerline. The scatter dose (μGy) was measured for each acquisition.

Effective Dose Calculation

The effective dose (ED) is an estimate of the stochastic risk for radiation. ED is the sum of different tissue exposures using

Table 2. System Scanning Parameters

Parameter	Device								
	Airo TruCT	Airo TruCT	Airo TruCT	Cios Spin	Cios Spin	Cios Spin	O-arm	O-arm	O-arm
Protocol name	Lumbar	Lumbar	Lumbar	Orthop spine	Orthop spine	Orthop spine	—	—	—
Organ program name	High-power modulated lumbar	30% mA Duke standard lumbar	15% Duke standard lumbar	Extra power obese	High quality	Standard	HD	Standard	Low dose
Study description	—	—	—	Orthop trauma	Orthop trauma	Orthop trauma	HD	Standard	Low dose
Convolution kernel	Sharp	Sharp	Sharp	Reduce noise	Standard	Standard	—	—	
Single image matrix size	512 × 512	512 × 512	512 × 512	512 × 512	512 × 512	512 × 512	512 × 512	512 × 512	512 × 512
Pixel size, mm	0.4355	0.373	0.3965	0.313	0.313	0.313	0.415	0.415	0.415
Slice thickness, mm	1	1	1	0.313	0.313	0.313	0.833	0.833	0.833
Total axial slices in volume	231	163	163	512	512	512	192	192	192
kVp	120	120	120	111	111	111	120	120	120
mA	113	35.7	25	—	—	—	80	63	40

Orthop, orthopedic; mA, milliamperes; HD, high-definition; kVp, kilovoltage peak.

specific tissue weighting factors to calculate a single number (in mSv), reflecting the overall risk. These factors vary by population-, age-, and sex-specific averages; hence, risks vary by individual. Because ED was calculated in a single cadaver model, the above variables were eliminated, resulting in a fair comparison of radiation exposure of each device.

Comparison of ED requires the acquisition dose measurements to be converted to mSv. The O-arm and Airo TruCT report dose via standard CT indices computed tomography dose index (CTDI) volume and dose length product. A standard abdominal K-factor (0.015) was used to convert dose length product to estimated ED in mSv.[8] The Cios Spin uses CBCT, measuring the dose in reference point air kerma (Ka,r) and dose area product. An ED/dose area product conversion factor of 0.29[9] was used to estimate the ED in mSv for comparison.

Subjective IQ

Axial images were categorized by device, screw segmentation, and dose level. Images were selected that visualized each screw at its midpoint; 36 images were randomized, blinded, and placed in a PowerPoint (Microsoft Corporation, Redmond, Washington, USA) presentation. Readers of diverse specialties (2 neurointerventional radiologists, 2 orthopedic surgeons, 1 dual-trained neuro and orthopedic surgeon, and 5 neurosurgeons) scored the identical 36 images in the same sequence with their native settings of windowing. Subjective IQ was scored on a Likert scale from 1 to 5 (1 = best, 5 = worst). Guidelines for rating included noise or graininess, sharpness, contrast, diagnostic confidence, and streak artifact. Each reader provided an overall score for each image.

Statistical Methods

IQ rating was considered a continuous variable for the primary analysis and comparison of IQ between devices. Descriptive statistics included mean, SD, median, first and third quartiles, and range for the scores. Based on all available data for each device, an SD estimate of 1.15 was assumed. Based on this estimate, the SD of a difference in imaging scores was expected to be 1.6, and the 80% confidence interval (CI) limits were given by (mean difference) ± 0.34 (N = 36). The estimated SD of the specific mean difference was used in each computation of the 80% CI. If the 80% CI for the difference was within (−0.84, 0.84), the subgroups were considered equivalent. If the 80% CI for the difference was outside this range, the subgroups were considered to differ in IQ. Mean differences in the scores were summarized and compared with the CI (−0.84, 0.84) to determine statistical significance. Pairwise comparisons were made among devices and dose levels and overall. All analyses were conducted using SAS 9.4 (SAS Institute Inc., Cary, North Carolina, USA).

A figure of merit (FOM) score was calculated by multiplying both subjective IQ and objective SD scores with the corresponding ED from that acquisition. Individual parameters favor low values; hence, the FOM combines several parameters into 1 index score, with lower values being better.

RESULTS

Images were selected with both screws in the field of view to show the worst-case streak artifacts for each device (Figure 1). A lower

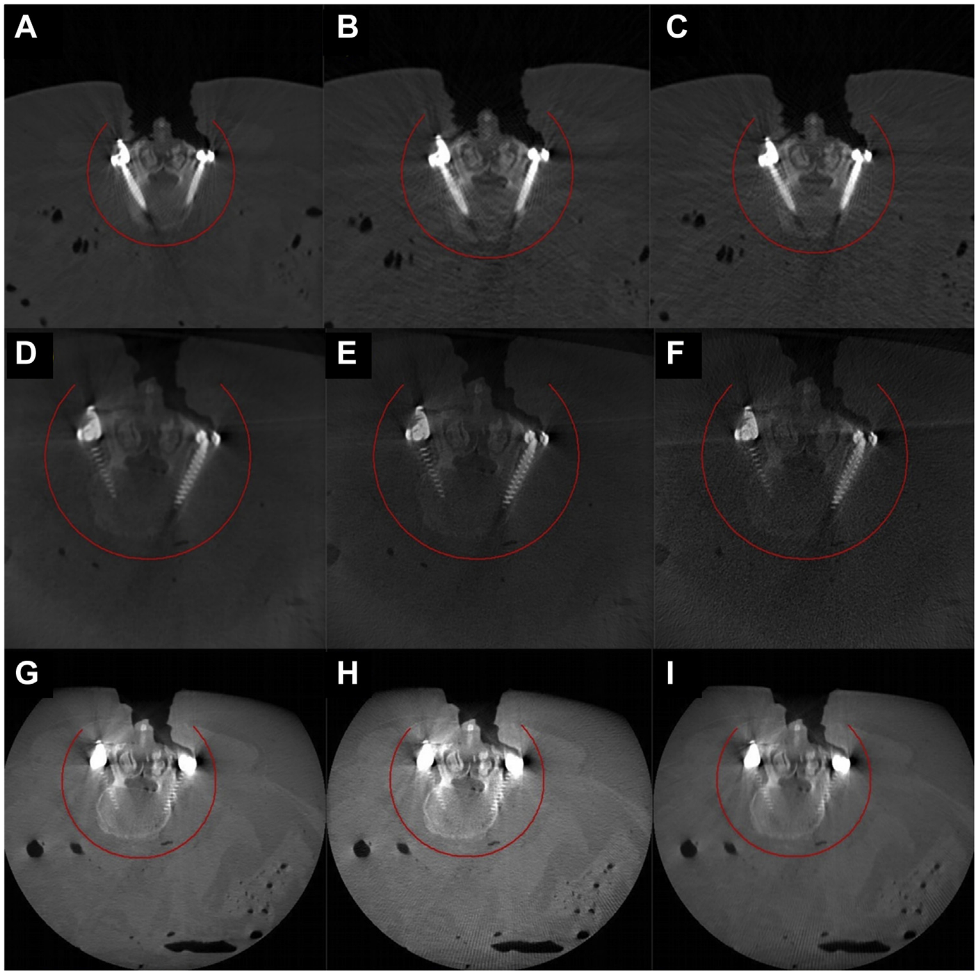

Figure 1. Axial images for all systems and all doses. (**A**–**C**) Airo TruCT: high (**A**), medium (**B**), and low (**C**) dose. (**D**–**F**) Cios Spin: high (**D**), medium (**E**), and low (**F**) dose. (**G**–**I**) O-arm: high (**G**), medium (**H**), and low dose (**I**).

SD indicates less pixel value variation and fewer streak artifacts in the image. The higher the SD, the greater the presence of streak artifacts worsening the IQ. The results for all vendors and values and peak SD are shown in Figure 2.

Scatter dose (μGy), ED, and machine doses in their specific metric (Ka,r and dose area product for Cios Spin; CTDI and dose length product for Airo TruCT and O-arm) are presented in Table 3. As expected, the scatter dose measured at 1 m increased proportionally with machine dose. Moving from low to medium doses increased the scatter dose by at least 50% in all devices. The medium to high progression increased dose by lower increments between 13% and 37%. Airo TruCT had the lowest ED at a low dose of 1.6 mSv, followed by Cios Spin at 1.9 mSv. The O-arm ED was roughly double the Airo TruCT at 3.3 mSv.

Before analysis, all IQ scores were analyzed for interrater reliability to identify outliers. One outlier was identified (reader 3), and we subsequently removed the corresponding scores from analysis. Images were blinded and then scored 1 (best) to 5 (worst). See Appendix A for a summary of ratings and descriptive statistics for all readers. A histogram (Figure 3) of the image scores by device, with the total percentage of 1s and 2s representing better IQ, shows the Cios Spin at 56%, the Airo TruCT at 31.48%, and the O-arm at 25.9%.

The best IQ scores (lower numbers) within devices were 2.22 for the Airo TruCT at a low dose, 2.22 for the O-arm at a high dose, and 1.44 for the Cios Spin device at a medium dose (Figure 4). Differences in IQ in pairwise comparison of dose levels within devices are shown in Table 4. The best IQ scores across devices are shown in Figure 5, with the corresponding differences in IQ in pairwise comparison in Table 5.

The comparisons of ED and subjective and objective IQ results are complex. FOM was used to combine subjective and objective IQ scores with their corresponding ED from that acquisition. The best (lowest) FOM scores were for the Airo TruCT low dose,

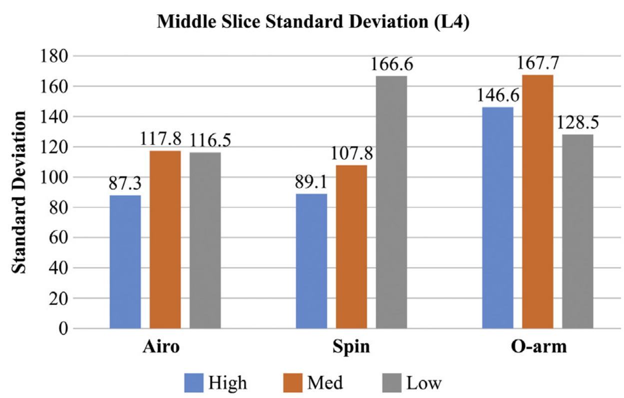

Figure 2. Peak scatter dose measurements for Airo TruCT, Cios Spin, and O-arm and all dose protocols.

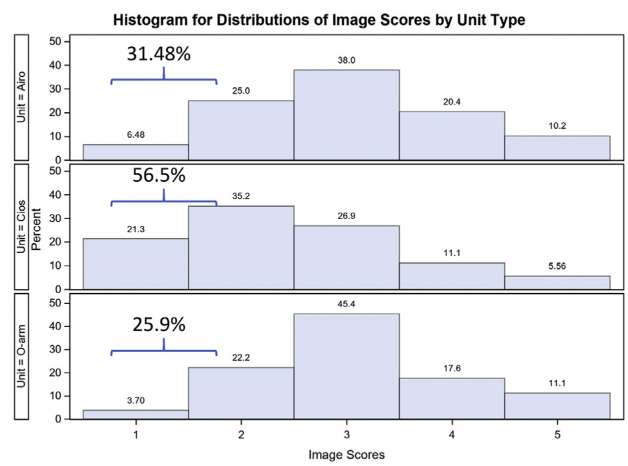

Figure 3. Histogram for distributions of image scores by unit type: Airo TruCT, Cios Spin, and O-arm. Percentages indicate the total percentage of good scores (1s and 2s).

followed by the Cios Spin medium dose and low dose. The highest FOM scores were for the O-arm high dose and medium dose, followed by the Airo TruCT high dose (**Figure 6**).

DISCUSSION

Radiation exposure in spine surgery is a relevant topic. Health care professionals who do not have sufficient knowledge concerning these topics may not be able to perform the risk/benefit analysis in clinical practice and thereby may expose themselves and their patients to the harmful effects of radiation.[10] Phantom studies, while accurate, repeatable, and with no institutional review board requirements, have limited clinical relevance for surgeons.[11-20] However, few studies exist in the literature that have simultaneously examined IQ and radiation dose in patients.[12,21,22] Patients with a larger body habitus require greater radiation dose to yield adequate IQ. Subsequently, multipatient studies comparing dose and/or IQ may be misleading. The aim of this study was to provide an accurate patient and operator dose comparison of the corresponding IQ impact across 3 different devices in a single cadaver model.

Our dose findings were consistent with similar previous phantom studies. Nelson et al.[23] found higher radiation levels in phantoms with O-arm and portable x-ray, as opposed to C-arm fluoroscopy. Moore et al.[24] compared radiation exposure (ED) among fluoroscopy, multidetector CT, and 2 mobile CT systems using a phantom 2- and 4-level fusion model. The ED range, from highest to lowest, was multidetector CT, mobile CT, and fluoroscopy. However, IQ was not assessed by either Nelson et al.[23] or Moore et al.[24]

Table 3. Dose Data From Machines, Scatter Dose, and Effective Dose

	Device								
Dose Data	**Airo TruCT**	**Airo TruCT**	**Airo TruCT**	**Cios Spin**	**Cios Spin**	**Cios Spin**	**O-arm**	**O-arm**	**O-arm**
Dose protocol	High	Med	Low	High	Med	Low	High	Med	Low
Dose data from machines									
Ka,r, mGy	—	—	—	119.95	103.61	48.6	—	—	—
DAP, µGy • m^2	—	—	—	1593.78	1376.67	645.68	—	—	—
CTDIvol, mGy	22.88	7.22	5.06	—	—	—	41.16	27.47	13.74
DLP, mGy • cm	645	154.6	108.2	—	—	—	658.3	439.4	219.7
Operator dose measured (scatter)									
Scatter dose @ 1 m, µGy	200	45.8	31.8	55.9	48.7	21.7	104.5	67.3	33.9
Effective dose, mSv	9.7	2.3	1.6	4.6	4.0	1.9	9.9	6.6	3.3

Med, medium; Ka,r, reference point air kerma; DAP, dose area product; CTDIvol, computed tomography dose index volume; DLP, dose length product.

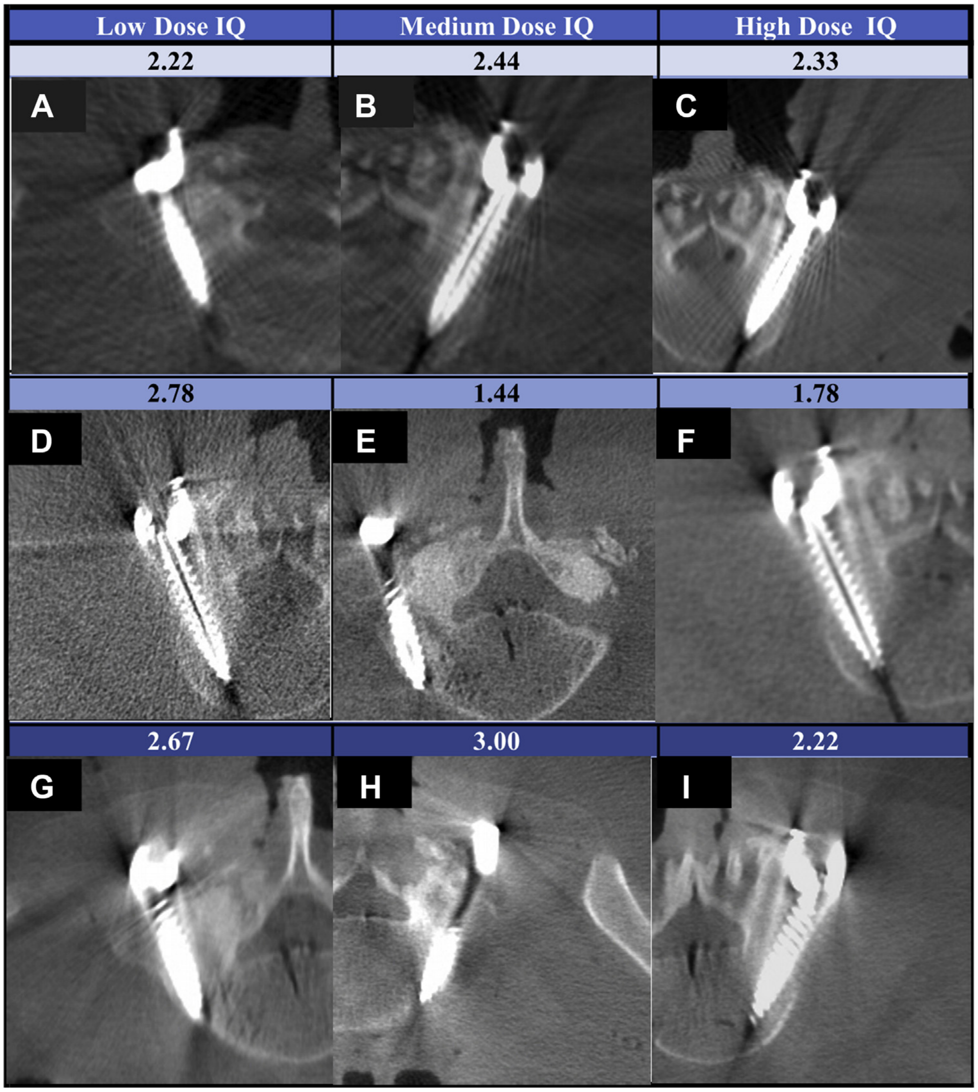

Figure 4. Best image quality score and corresponding image by dose per device. (**A**–**C**) Airo TruCT: low 2.22 (**A**), medium 2.44 (**B**), and high 2.33 (**C**). (**D**–**E**) Cios Spin: low 2.78 (**D**), medium 1.44 (**E**), and high 1.78 (**F**). (**G**–**I**) O-arm: low 2.67 (**G**), medium 3.00 (**H**), and high 2.22 (**I**). IQ, image quality.

Despite various approaches to reduce artifacts (high peak voltage, high tube current, collimation, image reconstruction), streaking from metal implants remains problematic. In this study, streak artifacts were measured using the SD of pixel data in the middle slice at L4 of each image. This was evident in the results with the highest SD score (worst image) corresponding to the worst IQ scores within each vendor. The best IQ scores within each vendor, however, did not have the lowest SD, but were all the midrange SD scores.

Regarding dose, surgeons are familiar with machine dose—the dose the equipment detects and is typically recorded in the patient chart or saved with the images. Machine dose does not reflect patient or operator dose. In this study, a direct comparison of machine dose was not possible owing to differences in image acquisition, reconstruction strategies, and dose metrics among the systems.

The Cios Spin and O-arm record machine dose in mGy; however, the Cio Spin measures Ka,r, and the O-arm measures CTDI volume. On medium-dose protocols, the machine dose of the Cios Spin (Ka,r) was 103.61 mGy, and the O-arm (CTDI volume) was 27.47 mGy. Given the same units, mGy, without understanding the metric (air kerma vs. CTDI volume), leads to an erroneous conclusion that the O-arm has a lower dose. ED is a surrogate patient dose estimate that can be used to gauge risk from stochastic effects and compares similar technologies and procedures using different technologies for the same medical examination. At the medium dose, the ED for the Cios Spin was 4.0 mSv, and the ED for the O-arm was 6.6 mSv.

Table 4. Pairwise Comparison of Dose Levels within Devices

Device	Dose Protocol Compared	Mean Difference	SD	80% CI
Airo TruCT	High/Med	−0.22	1.04	−0.54, 0.09
	High/Low	0.22	1.10	−0.11, 0.58
	Low/Med	−0.44	1.03	−0.76, −0.13
Cios Spin	High/Med	0.28	1.03	−0.04, 0.59
	High/Low*	−0.61	1.07	−0.94, −0.29
	Low/Med*	0.89	1.08	0.56, 1.22
O-arm	High/Med*	−0.92	0.94	−1.20, −0.63
	High/Low*	−0.64	0.87	−0.90, −0.37
	Low/Med	−0.28	0.97	−0.57, 0.02

SD, standard deviation; CI, confidence interval; Med, medium.
*Difference in image quality outside the CI. There was no difference in image quality across doses for Airo TruCT. The high and medium doses had better image quality compared with the low dose for Cios Spin. High dose had better image quality compared with the low and medium doses for O-arm.

The Airo TruCT had the lowest ED on low-dose protocols at 1.6 mSv, followed by the Cios Spin at 1.9 mSv. The O-arm and the Airo TruCT had the highest ED on high-dose settings at 9.9 mSv and 9.7 mSv. These measurements are directly comparable, as the same specimen was imaged. For all systems, moving from a low dose to a medium dose essentially doubles the ED. Thus, the benefits to the patient of an improved image must be weighed against the risk of doubling the radiation dose that the patient receives.

The purpose of this article was to provide an accurate comparison of radiation dose across imaging systems and the impact on IQ. For the Airo TruCT, there was no difference in IQ across high-, medium-, and low-dose settings on the cadaver, even though we found a 6-fold increase in radiation dose between the low- and high-dose settings. In contrast, differences in IQ were observed for both the Cios Spin (2.4×) and the O-arm (3×) between low- and high-dose settings. In this case, a higher dose might avoid additional acquisitions owing to poor visualization or screw misalignment and thus may be warranted.

Scatter radiation, also a uniform measure, is secondary radiation from an object intercepting the primary beam, resulting in operator exposure. The amount of scatter radiation at 1 m from either side of the patient will be 0.1% of the intensity of the primary x-ray beam.[25] Scatter dose can be calculated at any distance from the source using the inverse square law, which states that if the distance away from an unshielded radiation source is doubled, the dose is reduced by a factor of 4. Using the distance from the x-ray tube, the scatter dose to the personnel (i.e., anesthesiologist, circulating nurse, technologist, and surgeon) can be estimated. For comparison, at the medium dose setting, the scatter radiation (μGy) for the Airo TruCT, Cios Spin, and O-arm was 45.8 μGy, 48.7 μGy, and 67.3 μGy, respectively. Changing to a low-dose protocol reduces personnel exposure by 31% for the Airo TruCT, 55% for the Cios Spin, and 50% for the O-arm.

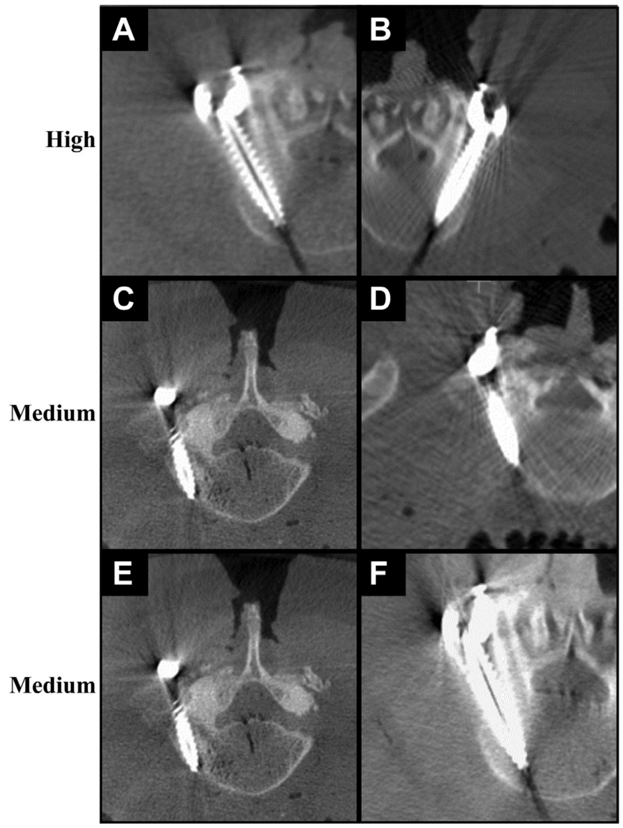

Figure 5. Image comparisons across devices by dose and image quality score. Lower score indicates the better image. (**A** and **B**) High dose: Cios Spin (1.78) (**A**) and Airo TruCT (2.33) (**B**). (**C** and **D**) Medium dose: Cios Spin (1.44) (**C**) and Airo TruCT (2.44) (**D**). (**E** and **F**) Medium dose: Cios Spin (1.44) (**E**) and O-arm (3.11) (**F**).

Table 5. Pairwise Comparison by Dose Levels Across Devices

Dose Protocol	Devices Compared	Mean	SD	80% CI
High dose	Airo TruCT/Cios Spin*	0.69	1.06	0.37, 1.02
	Airo TruCT/O-arm	0.44	0.98	0.14, 0.74
	Cio Spin/O-arm	−0.25	0.93	−0.53, 0.03
Med dose	Airo TruCT/Cios Spin*	1.19	1.00	0.89, 1.50
	Airo TruCT/O-arm	−0.25	1.00	−0.55, 0.05
	Cios Spin/O-arm*	−1.44	1.03	−1.76, −1.13
Low dose	Airo TruCT/Cios Spin	−0.14	1.11	−0.48, 0.20
	Airo TruCT/O-arm	−0.42	1.00	−0.72, −0.11
	Cios Spin/O-arm	−0.2	1.02	−0.59, 0.03

SD, standard deviation; CI, confidence interval; Med, medium.
*Difference in image quality. On high dose and medium doses, Cios Spin had better image quality than Airo TruCT. The Cios Spin had better image quality than the O-arm on medium dose, and no differences were noted across vendors on low dose.

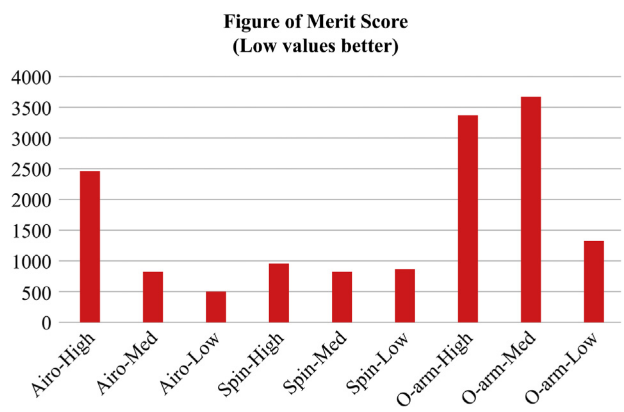

Figure 6. Figure of merit scores calculated by multiplying the standard deviation objective image quality scores, effective dose, and subjective image quality scores. Med, medium.

Additional methods to reduce scatter include shielding, the use of grids, and leaving the room during imaging. These methods rely on individual compliance for effectiveness, but the surgeon's request to use a dose reduction protocol benefits all.

While image-guided procedure volumes have been increasing, radiation awareness and education have not kept pace. A potential cause is the disconnect between exposure and knowledge about the amount of exposure per procedure.[5] However, numbers presented in isolation are difficult to relate to everyday use. Although geography dependent, the average natural background radiation exposure per individual is approximately 2.4 mSv a year.[26] The O-arm exceeds this value at all dose protocols in 1 scan. The Cios Spin exceeds it on high- and medium-dose protocols, and the Airo TruCT exceeds it on high-dose protocols.

Most institutions do not have access to multiple intraoperative imaging vendors. As procedure volumes increase, surgeons are increasingly involved in evaluating new imaging equipment as well as purchasing decisions. Radiation safety, including the dose and exposure of staff and patients in the operating room, is receiving increased attention.[27,28] Looking at IQ across vendors, on low-dose settings, no differences were noted; however, the ED of the O-arm (3.3 mSv) was double that of the Airo TruCT (1.6 mSv). While these numbers seem small, radiation exposure from scatter and direct exposure during spine surgery are far from negligible, and the carcinogenic effects are cumulative over the life span of the surgeon.[29-31] Thus, the lifetime risk of developing a malignancy can be reduced by small changes in the amount of cumulative radiation received.[32] Understanding the impact of device and protocol selection illustrates this point.

In general, the FOM is used to characterize the performance of a device, system, or method relative to its alternatives. The FOM scores calculated from IQ and ED represent both risk and benefit. This is perhaps the greatest data point from a surgeon's perspective, as it represents the best benefit (IQ) with the least corresponding risk (ED). The order of best to worst is as follows: Airo TruCT low, Cios Spin medium, Airo TruCT medium, Cios Spin low, Cios Spin high, O-arm low, Airo TruCT high, O-arm high, and O-arm medium.

Limitations

One study limitation was lower interrater agreement. This was most likely due to readers' varying degrees of experience with the devices, potentially resulting in familiarity bias when scoring. The subjective measurement for IQ was a composite score based on noise or graininess, sharpness, contrast, diagnostic confidence, and artifacts or streaks. The objective measure computed the SD of the pixel values assessing streak artifacts only, which may account for the variability. The use of this methodology as an objective measure to assess IQ holds promise; however, further research to draw accurate conclusions is required.

CONCLUSIONS

As the primary user, surgeons must apply a risk/benefit analysis balancing the operative imaging requirements while limiting radiation exposure to staff and patients. The data presented in this study illustrate the relationship between IQ and dose, heighten awareness of manufacturer dose reduction capabilities, and may enable risk evaluation and reduction in clinical practice.

CRediT AUTHORSHIP CONTRIBUTION STATEMENT

Norah Foster: Investigation, Formal analysis, Writing – original draft, Writing – review & editing. **Christopher Shaffrey:** Conceptualization, Methodology, Writing – review & editing. **Avery Buchholz:** Conceptualization, Methodology, Investigation, Writing – review & editing. **Raymond Turner:** Conceptualization, Methodology, Writing – review & editing. **Lexie Zidanyue Yang:** Formal analysis. **Donna Niedzwiecki:** Formal analysis. **Allen Goode:** Conceptualization, Methodology, Investigation, Formal analysis, Writing – original draft, Writing – review & editing.

ACKNOWLEDGMENTS

The authors thank Imalogix (Bryn Mawr, Pennsylvania, USA) for their assistance with DICOM images and Jennifer Schaadt for project administration and oversight of this research.

REFERENCES

1. NCRP Report No. 116. Limitation of exposure to ionizing radiation. Available at: https://ncrponline.org/publications/reports/ncrp-reports-116/. Accessed May 13, 2021.
2. Occupational Safety and Health Administration. 1910.1096—ionizing radiation. Available at: https://www.osha.gov/laws-regs/regulations/standardnumber/1910/1910.1096/. Accessed May 11, 2021.
3. United States Nuclear Regulatory Committee. Doses in our daily lives. Available at: https://www.nrc.gov/about-nrc/radiation/around-us/doses-daily-lives.html/. Accessed February 22, 2021.
4. Oddy MJ, Aldam CH. Ionising radiation exposure to orthopaedic trainees: the effect of sub-specialty training. *Ann R Coll Surg Engl*. 2006;88:297-301.
5. Godzik J, Mastorakos G, Nayar G, et al. Surgeon and staff radiation exposure in minimally invasive spinal surgery: prospective series using a personal dosimeter. *J Neurosurg Spine*. 2020;32:817-823.

6. Komlosi P, Grady P, Smith S, et al. Evaluation of monoenergetic imaging to reduce metallic instrumentation artifacts in computed tomography of the cervical spine. *J Neurosurg Spine*. 2015;22:34-38.

7. Komlosi P, Zhang Y, Leiva-Salina C, et al. Adaptive statistical iterative reconstruction reduces patient radiation dose in neuroradiology CT studies. *Neuroradiology*. 2014;56:187-193.

8. National Council of Protection in Radiation. NCRP report No. 160. Ionizing radiation exposure of the population of the United States. *J Radiol Prot*. 2009;29:465.

9. Hwang Y, Tsai H, Lin Y, et al. Investigations of organ and effective doses of abdominal cone-beam computed tomography during transarterial chemoembolization using Monte Carlo simulation. *BMC Med Imaging*. 2018;18:2-8.

10. Zekioğlu A, Parlar S. Investigation of awareness level concerning radiation safety among healthcare professionals who work in a radiation environment. *J Radiat Res Appl Sci*. 2021;14:1-8.

11. Santos JS, Uusi-Simola J, Kaasalainen T, Aho P, Venermo M. Radiation doses to staff in a hybrid operating room: an anthropomorphic phantom study with active electronic dosimeters. *Eur J Vasc Endovasc Surg*. 2020;59:654-660.

12. Konst B, Nøtthellen J, Bilet E, Båth M. Radiographic and fluoroscopic x-ray systems: quality control of the x-ray tube and automatic exposure control using theoretical spectra to determine air kerma and dose to a homogenous phantom. *J Appl Clin Med Phys*. 2021;22:204-218.

13. Paruccini N, Villa R, Oberhofer N, et al. A single phantom, a single statistical method for low-contrast detectability assessment. *Phys Med*. 2021;91:28-42.

14. Chiang HW, Wu RW, Yin TC, Li JH, Wang YS, Lin LH. Occupational radiation exposure of orthopedists at different locations during pedicle screw insertion: an anthropomorphic phantom study. *Technol Health Care*. 2021;29:211-219.

15. Legerstee IW, Oosterveer TT, Molenaar MA, et al. Scattered radiation during osteosynthesis of the distal radius: a phantom study. *J Radiol Imaging*. 2021;5:1-4.

16. Naseri Y, Hubbe U, Scholz C, Brönner J, Krüger MT, Klingler JH. Radiation exposure of a mobile 3D C-arm with large flat-panel detector for intraoperative imaging and navigation—an experimental study using an anthropomorphic Alderson phantom. *BMC Med Imaging*. 2020;20:96.

17. Metaxas VI, Messaris GA, Gatzounis GD, Panayiotakis GS. Optimisation of patient dose and image quality in fluoroscopically guided cervical spine surgery: a phantom-based study. *Radiat Prot Dosimetry*. 2019;184:237-247.

18. Chang CY, Simeone FJ, DeLorenzo MC, Palmer WE, Bredella MA, Huang AJ. Dose reduction for fluoroscopically guided injections: phantom simulation and patient procedures. *Skeletal Radiol*. 2018;47:223-231.

19. Awikunprasert P, Chandaeng T, Kuepitak K, Pungkun V. Radiation dose and dose distribution from fluoroscopy: phantom study. *Srinagarind Med J*. 2019;34:565-573.

20. Johnson PB, Geyer A, Borrego D, Ficarrotta K, Johnson K, Bolch WE. The impact of anthropometric patient-phantom matching on organ dose: a hybrid phantom study for fluoroscopy guided interventions. *Med Phys*. 2011;38:1008-1017.

21. Prasarn ML, Coyne E, Schreck M, Rodgers JD, Rechtine GR. Comparison of image quality and radiation exposure from C-arm fluoroscopes when used for imaging the spine. *Spine (Phila Pa 1976)*. 2013;38:1401-1404.

22. Nachabe R, Strauss K, Scheuler B, Bydon M. Radiation dose and image quality comparison during spine surgery with two different, intraoperative 3D imaging navigation systems. *J Appl Clin Med Phys*. 2019;20:136-145.

23. Nelson E, Monazzam S, Kim K, et al. Intraoperative fluoroscopy, portable x-ray, and CT: patient and operating room personnel radiation exposure in spinal surgery. *Spine J*. 2014;14:2985-2991.

24. Moore B, Womak K, Nguyen, et al. Patient dose comparison for intraoperative imaging devices used in orthopedic lumbar spinal surgery. *J Am Acad Orthop Surg Glob Res Rev*. 2018;2:e030.

25. Health Physics Society. Answer to question #11780 submitted to "ask the experts." Available at: https://hps.org/publicinformation/ate/q11780.html/. Accessed December 15, 2021.

26. International Atomic Energy Agency. Radiation in everyday live. Available at: https://www.iaea.org/Publications/Factsheets/English/radlife/. Accessed December 15, 2021.

27. Kim CW, Lee YP, Taylor W, et al. Use of navigation-assisted fluoroscopy to decrease radiation exposure during minimally invasive spine surgery. *Spine J*. 2008;8:584-590.

28. Medtronic. Dose considerations O-Arm surgical imaging system. Available at: https://www.medtronic.com/us-en/healthcare-professionals/products/neurological/surgical-imaging-systems/o-arm/dose-considerations.html/. Accessed December 16, 2021.

29. Centers for Disease Control and Prevention. ALARA—as low as reasonably achievable. Available at: https://www.cdc.gov/nceh/radiation/alara.html/. Accessed December 18, 2021.

30. Mroz TE, Abdullah KG, Steinmetz MP, et al. Radiation exposure to the surgeon during percutaneous pedicle screw placement. *J Spinal Disord Tech*. 2011;24:264-267.

31. Smith HE, Welsch MD, Sasso RC, et al. Comparison of radiation exposure in lumbar pedicle screw placement with fluoroscopy vs computer-assisted image guidance with intraoperative three-dimensional imaging. *J Spinal Cord Med*. 2008;31:532-537.

32. Pennington Z, Cottrill E, Westbroek EM, et al. Evaluation of surgeon and patient radiation exposure by imaging technology in patients undergoing thoracolumbar fusion: systematic review of the literature. *Spine J*. 2019;19:1397-1411.

Conflict of interest statement: This research was supported by the National Center for Advancing Translational Sciences of the National Institutes of Health under Award Number UL1TR002553. R. Turner is a consultant for Siemens Healthineers and Medtronic. A. Goode is a physics key opinion leader for Siemens Healthineers.

The content of this article is solely the responsibility of the authors and does not necessarily represent the official views of the National Institutes of Health.

Received 16 October 2021; accepted 27 December 2021

Citation: World Neurosurg. (2022) 160:e142-e151.
https://doi.org/10.1016/j.wneu.2021.12.103

Journal homepage: ***www.journals.elsevier.com/world-neurosurgery***

Available online: ***www.sciencedirect.com***

APPENDIX

Appendix A. Mean (SD) and Median (Q1, Q3) Rating Scores for Each Rater by Unit Type and Radiation Dose Level

	Airo TruCT			Cios Spin			O-arm			
	Low (n = 4)	Med (n = 4)	High (n = 4)	Low (n = 4)	Med (n = 4)	High (n = 4)	Low (n = 4)	Med (n = 4)	High (n = 4)	Total (n = 36)
Reader 1										
Mean (SD)	1.8 (0.5)	2.5 (1.0)	2.5 (0.6)	1.8 (0.5)	1.0 (0.0)	2.0 (0.8)	2.5 (1.0)	2.8 (0.5)	2.3 (0.5)	2.1 (0.8)
Median (Q1, Q3)	2.0 (1.5, 2.0)	3.0 (2.0, 3.0)	2.5 (2.0, 3.0)	2.0 (1.5, 2.0)	1.0 (1.0, 1.0)	2.0 (1.5, 2.5)	2.0 (2.0, 3.0)	3.0 (2.5, 3.0)	2.0 (2.0, 2.5)	2.0 (2.0, 3.0)
Reader 2										
Mean (SD)	2.0 (0.8)	2.8 (0.5)	2.0 (0.8)	2.8 (0.5)	2.8 (1.0)	2.5 (1.0)	3.5 (0.6)	4.0 (0.8)	3.0 (0.0)	2.8 (0.9)
Median (Q1, Q3)	2.0 (1.5, 2.5)	3.0 (2.5, 3.0)	2.0 (1.5, 2.5)	3.0 (2.5, 3.0)	2.5 (2.0, 3.5)	2.0 (2.0, 3.0)	3.5 (3.0, 4.0)	4.0 (3.5, 4.5)	3.0 (3.0, 3.0)	3.0 (2.0, 3.0)
Reader 4										
Mean (SD)	3.3 (1.0)	4.0 (0.8)	3.5 (1.7)	4.3 (1.0)	3.0 (1.6)	3.0 (1.8)	3.0 (0.8)	2.8 (1.0)	1.8 (1.0)	3.2 (1.3)
Median (Q1, Q3)	3.5 (2.5, 4.0)	4.0 (3.5, 4.5)	4.0 (2.5, 4.5)	4.5 (3.5, 5.0)	3.0 (2.0, 4.0)	3.0 (1.5, 4.5)	3.0 (2.5, 3.5)	2.5 (2.0, 3.5)	1.5 (1.0, 2.5)	3.0 (2.0, 4.0)
Reader 5										
Mean (SD)	4.0 (0.8)	4.0 (1.4)	4.0 (1.2)	2.0 (1.2)	1.5 (1.0)	1.3 (0.5)	4.0 (1.2)	4.0 (1.2)	3.5 (1.0)	3.1 (1.5)
Median (Q1, Q3)	4.0 (3.5, 4.5)	4.5 (3.0, 5.0)	4.0 (3.0, 5.0)	2.0 (1.0, 3.0)	1.0 (1.0, 2.0)	1.0 (1.0, 1.5)	4.0 (3.0, 5.0)	4.0 (3.0, 5.0)	3.0 (3.0, 4.0)	3.0 (2.0, 5.0)
Reader 6										
Mean (SD)	3.5 (1.3)	3.3 (1.0)	3.8 (0.5)	2.5 (0.6)	1.8 (1.0)	2.0 (0.8)	3.0 (1.4)	4.8 (0.5)	2.5 (0.6)	3.0 (1.2)
Median (Q1, Q3)	3.5 (2.5, 4.5)	3.5 (2.5, 4.0)	4.0 (3.5, 4.0)	2.5 (2.0, 3.0)	1.5 (1.0, 2.5)	2.0 (1.5, 2.5)	2.5 (2.0, 4.0)	5.0 (4.5, 5.0)	2.5 (2.0, 3.0)	3.0 (2.0, 4.0)
Reader 7										
Mean (SD)	3.0 (0.8)	3.0 (0.0)	3.0 (0.0)	3.0 (0.8)	1.5 (0.6)	2.3 (0.5)	2.8 (0.5)	2.3 (0.5)	1.8 (0.5)	2.5 (0.7)
Median (Q1, Q3)	3.0 (2.5, 3.5)	3.0 (3.0, 3.0)	3.0 (3.0, 3.0)	3.0 (2.5, 3.5)	1.5 (1.0, 2.0)	2.0 (2.0, 2.5)	3.0 (2.5, 3.0)	2.0 (2.0, 2.5)	2.0 (1.5, 2.0)	3.0 (2.0, 3.0)
Reader 8										
Mean (SD)	3.3 (1.3)	3.8 (1.3)	2.5 (1.7)	4.5 (0.6)	2.8 (1.0)	3.5 (0.6)	3.8 (1.0)	3.0 (0.8)	2.5 (1.3)	3.3 (1.2)
Median (Q1, Q3)	3.0 (2.5, 4.0)	4.0 (3.0, 4.5)	2.0 (1.5, 3.5)	4.5 (4.0, 5.0)	2.5 (2.0, 3.5)	3.5 (3.0, 4.0)	3.5 (3.0, 4.5)	3.0 (2.5, 3.5)	2.5 (1.5, 3.5)	3.0 (2.0, 4.0)
Reader 9										
Mean (SD)	2.0 (0.8)	2.8 (1.0)	2.5 (0.6)	3.5 (0.6)	2.0 (0.8)	2.0 (0.8)	3.0 (0.0)	4.0 (0.8)	3.0 (0.0)	2.8 (0.9)
Median (Q1, Q3)	2.0 (1.5, 2.5)	2.5 (2.0, 3.5)	2.5 (2.0, 3.0)	3.5 (3.0, 4.0)	2.0 (1.5, 2.5)	2.0 (1.5, 2.5)	3.0 (3.0, 3.0)	4.0 (3.5, 4.5)	3.0 (3.0, 3.0)	3.0 (2.0, 3.0)
Reader 10										
Mean (SD)	2.5 (0.6)	3.3 (0.5)	3.5 (0.6)	2.3 (0.5)	2.3 (0.5)	2.5 (0.6)	3.5 (0.6)	4.0 (0.0)	3.0 (0.0)	3.0 (0.7)
Median (Q1, Q3)	2.5 (2.0, 3.0)	3.0 (3.0, 3.5)	3.5 (3.0, 4.0)	2.0 (2.0, 2.5)	2.0 (2.0, 2.5)	2.5 (2.0, 3.0)	3.5 (3.0, 4.0)	4.0 (4.0, 4.0)	3.0 (3.0, 3.0)	3.0 (2.0, 3.5)
All Readers*										
Mean (SD)	2.8 (1.1)	3.3 (1.0)	3.0 (1.1)	2.9 (1.1)	2.1 (1.0)	2.3 (1.0)	3.2 (0.9)	3.5 (1.0)	2.6 (0.8)	2.9 (1.1)
Median (Q1, Q3)	3.0 (2.0, 3.5)	3.0 (3.0, 4.0)	3.0 (2.0, 4.0)	3.0 (2.0, 4.0)	2.0 (1.0, 3.0)	2.0 (2.0, 3.0)	3.0 (3.0, 4.0)	3.5 (3.0, 4.0)	3.0 (2.0, 3.0)	3.0 (2.0, 4.0)

SD, standard deviation; Q, quartile.
*n = 36 for each dose level (4 images × 9 readers), N = 324 for total (4 images × 9 readers × 3 dose levels × 3 devices).